Journal of Engineering and Technology

ISSN 2180-3811 eISSN 2289-814X https://jet.utem.edu.my/jet/index

EFFECT OF MESH REFINEMENT ON VERTICAL AND LATERAL VELOCITY PROFILES OF THE WAKE FLOW BEHIND A SPIRE USING COMPUTATIONAL FLUID DYNAMIC (CFD)

M. A. Fitriady*[1,3], N. A. Rahmat*[1], A. F. Mohammad[2] and S. A. Zaki[2]

[1] Faculty of Technology Mechanical and Automotive Engineering, Universiti Malaysia Pahang (UMP), Pahang, Malaysia.

[2] Malaysia-Japan International Institute of Technology, Universiti Teknologi Malaysia (UTM), Kuala Lumpur, Malaysia.

[3] Research Center for Chemistry, Nasional Research and Innovation Agency (BRIN), Jakarta, Indonesia

corresponding: arifuddinK46@gmail.com, izzatulatikha@ump.edu.my

Article history:
Received Date: 15 November 2022
Revised Date: 31 March 2023
Accepted Date: 30 April 2023

Keywords:
Computational Fluid Dynamics,

Abstract— The application of CFD to simulate the phenomenon based on a wind tunnel experiment has been widely studied. A large number of cells may produce accurate results but requires a high computational load. In this study, the effect of mesh refinement on the vertical and lateral velocity profiles of the wake flow behind a single spire is discussed. Three different mesh refinement levels, i.e. coarse, medium and fine, each with 9 million, 12.7 million, and 16.9 million cells were applied to the computational domain. The standard *k-ε*

Mesh Refinement, Spire, Wind Tunnel, Velocity Profiles

model was used as turbulence model. The variable mesh was generated by using *blockMesh* and *snappyHexMesh* features in the OpenFoam® software. The results show that there is slightly difference between each case, which reduced as the distance increase in both vertical, and sreamwise direction. However, there is a significant difference in the time needed to complete the iteration for each case whereby the shortest time was obtained by the coarse case. Hence, it is more feasible to adopt the coarse case to simulate the wake flow behind a single spire

I. Introduction

CFD has been widely used to simulate flow-related phenomena based on wind tunnel experiments. Some of the latest studies were conducted by [1][2].

Nagawkar et. al used the standard *k-ε* turbulence model was used by [1] to analyse the wind flow around the imperial tower and the neighbouring structures in the residential-commercial area of south Mumbai, India. As a numerical model, an approximate plan with two 3-Bedroom Hall Kitchen (BHK) flats on each floor completed with surrounding buildings based on Google Earth data was used. The simulation found a stagnation point with nearly zero velocity on the windward side of the skyscraper, and the flow is channelled around the structures, resulting in an enhanced velocity on the side of the imperial tower. This phenomenon causes low pressure to develop to the leeward of the imperial tower, as indicated by the nearly zero velocity. The author claimed unequivocally that the low velocity is due to the creation of the wake. Furthermore, as the atmospheric boundary layer re-stabilizes, the greater the

streamwise distance results in the greater the wind velocity [1].

While Harun et. al used Large Eddies Simulation using the Pressure-Implicit with Splitting of Operators (PISO algorithm as the solver to observe the wind flow around the Petronas Twin Tower, Malaysia's tallest skyscraper. In the numerical domain, the author employed the full size of the towers. However, the author only took into account the primary part of the tower, which is the greatest piece of each tower with a diameter of *60 m* and a height of *250 m*. The simulation demonstrated that two vortical areas formed in the flow, one in between the two towers and the other downstream of the tower. The in-between vortices are much stronger, which is both larger in size and higher in velocity, than the downstream vortices because the downstream vortices are diminished by the freestream velocity. However, the in-between vortices exhibit less turbulence than the downstream vortices. [2].

A study utilizing a skyscraper in the middle of an urban environment can be replicated by using a single spire followed by a rough wall background in wind tunnel experiment. A comparison of vertical and lateral velocity profiles from a wind tunnel experiment using a single spire model and a CFD case using a real skyscraper model was reported, leading to a conclusion that the vertical velocity profiles generated by the single spire model have a similar trend as the one generated by the real skyscraper model. Furthermore, the mean lateral velocity profile exhibits a similar pattern [3].

Therefore, the velocity profiles of wind flow behind a quarter elliptic-wedge spire that is normally installed as a vortex generator inside a small-scaled boundary-layer wind tunnel were investigated in the present study. While using a high number of computational meshes or cells may produce accurate results, however, it needs a high computational load to complete [4]. Therefore, mesh optimization is required to obtain the best mesh quality while maintaining a low

computational load for accurate results in CFD studies comparable to wind tunnel experimental data. In this study, the effect of the mesh number on the velocity profiles generated by the CFD based on the wind tunnel case is discussed.

II. Methodology

This study was conducted using open-sourced CFD software, OpenFOAM®. The preparation for the CFD case consists of the numerical domain creation and the setup of the turbulence model. Upon the execution, *simpleFoam* was used as the solver of the simulation. Finally, post-processing i.e. data extraction was conducted using ParaView®. All these steps will be explained further.

A. Numerical Domain

The numerical domain consists of the wind tunnel model, the flat plate model, and the spire model. The wind tunnel model has a dimension of *0.3 m* (height) × *0.3 m* (width) × *3 m* (streamwise length). The flat plate was applied in the simulation based on the wind tunnel study [5]. A single quarter elliptic wedge spire, which has a height of *0.05 m* (*S*), a length of *0.025 m* (*0.5S*), and a width of *0.005 m* (*0.1S*), was applied in this study based on the previous study [6]–[8]. The wedge angle is 5.71° by default. The spire was installed at the upwind position in the center ($y = 0$) of the wind tunnel, *2S* from the leading edge of the flat plate [5].

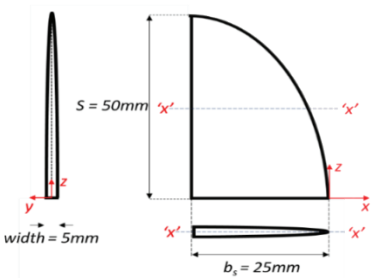

Figure 1: Schematic figure of a quarter elliptic-wedge spire model and its dimension

Figure 1 and Figure 2 present the layout of the dimension of the spire and the computational domain respectively. To observe the development and the recovery of the wake flow, the distribution of streamwise velocity was measured at eleven leeward positions (x_0) from the near wake regions of *0.5S, 1S, 3S,*

and *6S,* to far wake regions of *13S, 17S, 20S, 26S, 32S, 38S,* and *50S* for the vertical velocity profile. In addition, the lateral velocity profile was measured at some height variable i.e. *z=0.1S, 0.2S, 0.3S, 0.4S, 0.6S, 0.8S,* and *1.2S*, Table 1 summarized all the CFD variable conditions observed in this study.

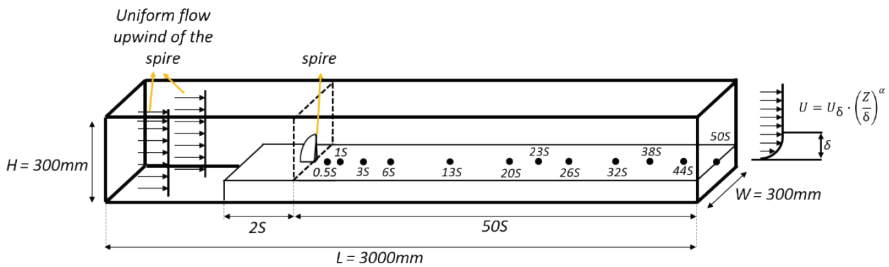

Figure 2: Schematic figure of the computational domain layout completed with the flat plate and the spire

Table 1: The CFD variable condition

	Near wake region	Far wake region
Standard *k-ε* turbulence model	Streamwise direction (x_0) : *0.5S, 1S, 3S,* and *6S*	Streamwise direction (x_0) : *13S, 20S, 26S, 32S, 38S,* and *50S*
	Vertical direction : *0.1S, 0.2S, 0.3S, 0.4S, 0.6S, 0.8S* and *1.2S*	

The 3D model is designed using open-source Computer-Aided Design (CAD) software i.e. FreeCAD®. Both the *blockMesh* utility and the *snappyHexMesh* utility were used to finalize the numerical domain. Figure 3 presents the block mesh scheme for the numerical domain consisting of four hexagonal-shaped blocks. Figure 4 and Figure 5 show the wire mesh view of the numerical domain and the 3-D spire model inside the domain, respectively.

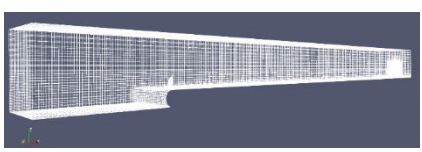

Figure 4: The wire mesh view of the numerical domain for the CFD simulation

In order to get various mesh densities, a variable mesh number, which is based on Table

2, was applied in the *blockMesh* scheme. This variable mesh number creates a significantly different mesh number, representing coarse, medium and fine cases for the lowest, medium and highest mesh numbers, respectively, after *snappyHexMesh* was executed as presented in Table 3. The *refinementBox* option was activated upon the execution of *snappyHexMesh* with level 10 in the surrounding area of the spire ($-1S \leq y \leq 1S$) along with the streamwise distance ($-2S \leq x_0 \leq 50S$) and vertical distance ($0 \leq z \leq 4S$).

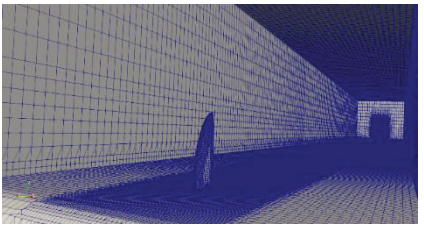

Figure 5: The internal view of the numerical domain showing the 3-D spire model

Table 2: The variable mesh number applied in the *blockMesh* scheme

Hexagonal	Mesh Density			Grading		
	x	*y*	*Z*	*x*	*y*	*z*
0 3 2 1 6 9 8 7	C = 106 M= 128 F = 150	C = 20 M= 24 F = 27	C = 11 M= 13 F = 5	C = M = F = 1	C = M = F = 1	C = M = F = 1
3 4 5 2 9 10 11 8	C = 53 M= 64 F = 75			C = M = F = 2		
6 9 8 7 12 15 14 13	C = 106 M= 128 F = 150	C = 20 M= 24 F = 27	C = 6 M= 7 F = 8	C = M = F = 1		
9 10 11 8 15 16 17 14	C = 53 M= 64 F = 75			C = M = F = 2		

C = Coarse, M = Medium, and F = Fine; *x, y,* and *z* are the axis

Table 3: The mesh density generated using the *snappyHexMesh* utility

Variable	Mesh Number
Coarse	9,068,182
Medium	12,758,227
Fines	16,911,390

B. Turbulence Model and Time Step Setting

The simulations were carried out using the well-known *Reynolds-Averaged Navier Stokes* (RANS) turbulence model i.e. standard k-ε model. The following initial conditions were applied; incoming flow speed ($U = 10\ ms^{-1}$), and the turbulence dissipation rate constant ($\varepsilon = 14.855\ m^2s^{-3}$). The simulations were run in parallel using eight processors with the time step of 1. The data was written and recorded every 50 s. The simulations were executed with the steady-state solver, *simpleFoam.*

The computation reached a steady state when the convergence point, which is usually defined prior to the simulation process, is achieved. In this study, the convergence of the steady-state simulation is justified based on the residual chart pattern, shown in Figure 6. Based on the residual charts, it can be stated that all cases achieved a steady state at 2000 iterations. Hence, the utilization of the latest time step data is valid. Since this is a steady state case, the data should not have any difference in time when the steady state is already achieved.

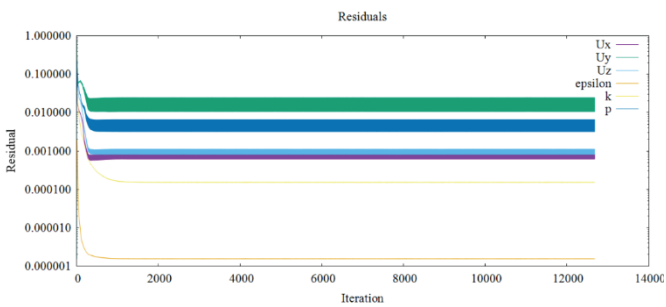

(a)

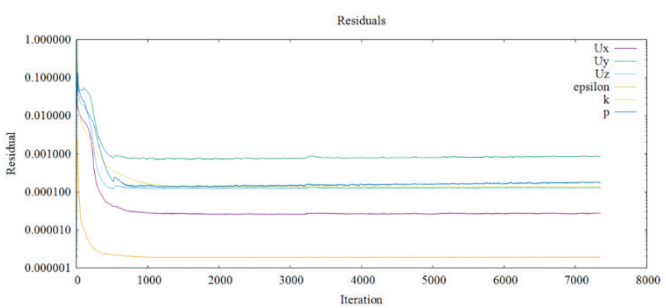

(b)

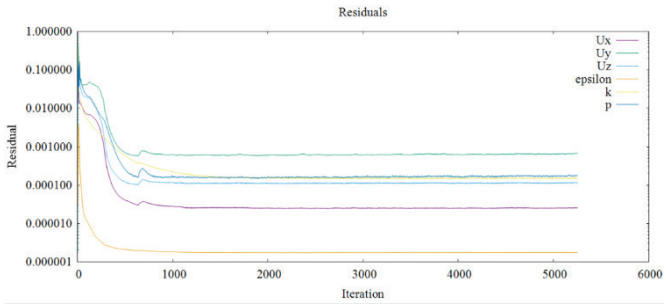

(c)

Figure 6: The residual plots for (a) coarse, (b) medium and (c) fine cases

C. Data Acquisition and Analysis

The analysis of the vertical and lateral velocity profile was done where both velocity profile data were extracted using the post-processing software, ParaView®. The numerical domain was sliced based on the distance in the streamwise direction (x_0) from $x_0 = 0.5S$ up to $x_0 = 50S$, and then plotted over line vertically at the center of the wind tunnel ($y = 0$) and horizontally according to the height variable from $z = 0.1S$ up to $z = 2S$ for vertical and lateral velocity profile respectively. The data were extracted for the latest time steps using the *save data* feature. The graphical plot and the discussion were based on these analyses. Some equations used in the analysis will be described in the corresponding subchapter.

III. Results and Discussion

The effect of mesh refinement was observed by comparing the velocity profile for each case. A vertical and lateral velocity profile was adopted to observe these effects. On top of that, the performance of each case, which was determined by the iteration speed, was also compared. All of these aspects were discussed in detail.

A. Vertical Velocity Profile

Figure 7 presents the normalized vertical velocity profile at the center of the lateral direction ($y=0$) of all simulation cases in several streamwise

directions. U/U_{ref} is the streamwise velocity (U) normalized by the reference velocity (U_{ref}) at $y=0$, and $z=2S$ for each streamwise position. The normalized vertical velocity is at the lowest value just above the ground, logarithmically increased as the vertical distance increased, and remained constant after some height.

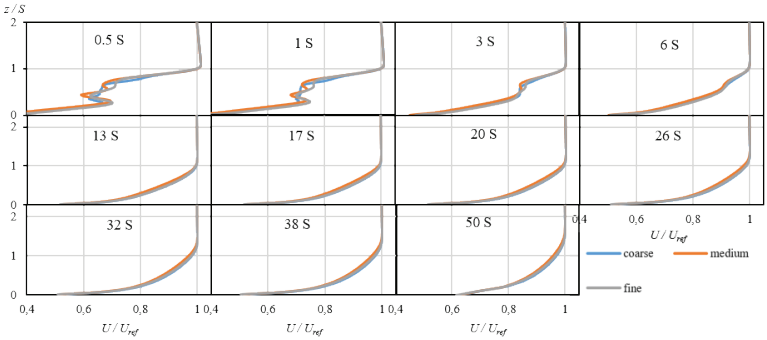

Figure 7: Normalized vertical velocity profiles at the center of the lateral direction ($y=0$) of all simulation cases. The vertical axis indicates the elevation normalized by the spire height S

It can be seen that the difference between the variables is not significant, indicated by the same height where the velocity turned into constant in all simulation ceases. However, each simulation case predicted a different fluctuation within the Boundary Layer Height (BLH) especially at the height of $0.6S \leq z_0 \leq 0.8S$ in the near wake region ($0.5S \leq x_0 \leq 6S$). Moreover, the fluctuation, and hence the difference, between each simulation case reduced as the streamwise distance increased. Referring to the far wake region ($13S \leq x_0 \leq 50S$), the fine case is more similar to the coarse case. The BLH development, which can be determined based on the vertical velocity profile, has a very important role in this study because it determines the wake flow structure at all streamwise positions. Since there are various methods in determining the BLH, this study adopts the one proposed by Kozmar et. al. who stated that the BLH is the height where the normalized vertical velocity is equal to

99.9% of the freestream velocity ($U/U_{ref}=0.999$) [9][10]. Figure 8 (a) presents BLH development with the streamwise distance of all simulation cases. It can be observed that all cases predict a similar trend of BLH. However, the coarse case prediction is more similar to the fine case. This phenomenon is presented in Figure 8 (b) which shows the BLH differences ($\Delta\delta$) between the cases. Based on Figure 8 (b), the $\Delta\delta$ of coarse-fine case is always less than 3% in all streamwise directions. On the other hand, $\Delta\delta$ of the medium-fine case is less than 3% only in the near wake region ($0.5S \leq x_0 \leq 13S$) while in the far wake region ($17S \leq x_0 \leq 50S$) the difference rose up to 7.32% at max value. Even though the BLH difference is within the tolerance (<10%) for all cases compared to the fine case, adopting the coarse case is more preferred due to the higher similarity to the fine case.

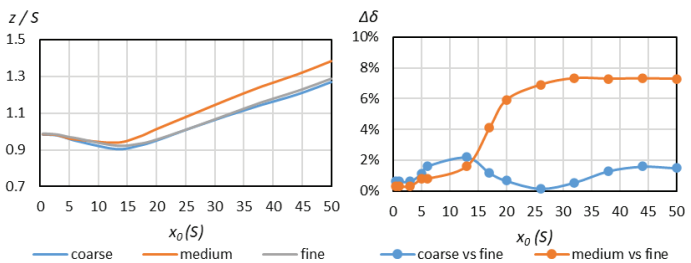

(a) (b)

Figure 8: (a) BLH development along streamwise distance of all simulation cases. The vertical axis indicates the elevation normalized by the spire height S; (b) the BLH difference (%) between coarse–fine and medium–fine

B. Lateral Velocity Profile

In order to observe the effect of mesh refinement on the vertical distance, the lateral velocity profile was conducted at several heights. Figure 9 shows the velocity distributions in the spanwise direction for several chosen heights at $x_0=0.5S$. The velocity was normalized based on Equation (1) as follows:

$$U_n(x,y,z) = \frac{U(x,y,z)}{U(x,y=1.6S,z=2S)} \quad (1)$$

The reference point is at y = 1.6S and $z = 2S$ where the effect of the spire should be minimal.

Based on Figure 9, the negative peak, which represents the reduced velocity due to the spire, can be observed at the center of the lateral direction in all vertical distances except $z = 2S$. There is a slight difference between all cases, especially within the BLH ($0.1S \leq z \leq 0.3S$), indicated by the layered graph with the lowest value predicted by the coarse case and the highest by the medium case, while the fine case was in-between the coarse and medium cases. These differences between all cases were reduced as the vertical distance increased. At the BLH, the negative peak predicted by all cases already overlapped to each other. In other words, there is no significant difference between the cases at and above the BLH in the vertical direction.

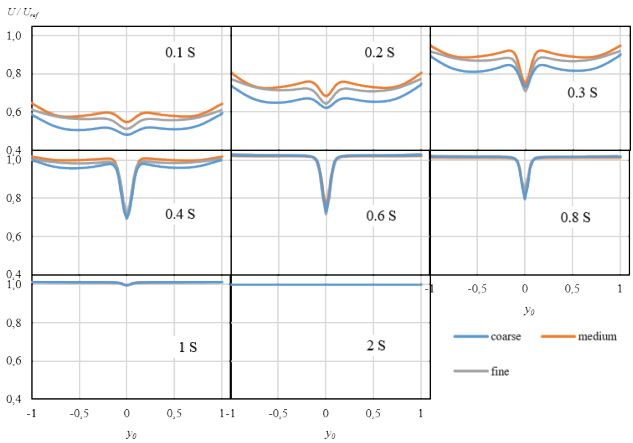

Figure 9: Normalized lateral velocity profiles at various heights (z_0=*0.1S, 0.2S, 0.3S, 0.4S, 0.6S, 0.8S, 1S,* and *2S*) of all simulation cases at x_0=*1S*

C. Performance Based on Iteration Speed

Moreover, the time needed by the case to execute the iterations is also an important aspect. The iteration speed was determined as the time needed by a single iteration in average (s/iteration) that was calculated based on Equation (2):

$$Iteration\ Speed = \frac{ExecutionTime}{Iteration\ Number} \quad (2)$$

Both *ExecutionTime* data and *iteration number* were extracted from the log file of each case.

Table 4 shows the iteration speed of coarse, medium, and fine cases.

Based on Table 4, it can be concluded that both coarse and medium case is faster by 227% and 138% compared to the fine case, respectively. This is as expected that the computational load is proportional to the mesh number. Since the coarse case has the least mesh number, it undoubtedly has the smallest computational load and hence the fastest iteration speed of all cases in this study.

Referring to the previous effect of mesh refinement, the coarse case is more preferred as it produces a similar prediction as the fine case with a significantly faster iteration speed. In other words, it is more feasible to adopt the coarse case in this study because of the similar result with significantly faster computation compared to the fine case.

Table 4: Iteration speed of all cases

Variable	Iteration Speed
Coarse	11 s/iteration
Medium	18 s/iteration
Fine	25 s/iteration

IV. Conclusion

A numerical study was conducted based on CFD using a wind tunnel model completed with a single quarter elliptic-wedge spire as the vortex generator to observe the effect of the mesh refinement on the velocity profile prediction as well as the performance of the case. Both vertical and lateral velocity profile was used to compare the prediction of variable case. Based on the vertical velocity profile, the fine case prediction has more similarity to the coarse case compared to the medium case. This is presented with the overlapped graph in BLH while the medium case is slightly overpredicted compared to both fine and coarse cases. Moreover, based on the lateral velocity profile, the difference between the cases can be observed within the BLH. In other words, the effect of mesh refinement is not significant at and above the BLH. On top of that, the performance of each case, which is determined by the iteration speed, was also compared. Based on the iteration speed,

both coarse case and medium cases are significantly faster than the fine case. Referring to the effect of mesh refinement as mentioned, the coarse case is more preferred as it produced a similar prediction as the fine case with a significantly faster iteration speed. In other words, it is more feasible to adopt the coarse case in this study because of the similar result but significantly faster compared to the fine case.

V. Acknowledgement

The authors gratefully acknowledge the research grant and financial support provided by the Ministry of Higher Education, MOHE (under the FRGS grant number: FRGS/1/2019/TK07/UMP/02/7 (RDU1901208) and Universiti Malaysia Pahang, UMP (under UMP grant number: RDU190375) also the MRS scholarship.

VI. References

[1] J. Nagawkar, S. Ghosh, R. Kataria, A. Nashit, and A. Deora, "Effect of skyscrapers on natural ventilation patterns and human comfort index in low-risebuildings - a CFD analysis over central Mumbai," *ARPN J. Eng. Appl. Sci.*, vol. 9, no. 3, pp. 293–295, 2014.

[2] Z. Harun, E. Reda, and S. Abdullah, "Large Eddy Simulation of the Wind Flow Over Skyscrapers," *Recent Adv. Mech. Mech. Eng.*, vol. 15, pp. 72–79, 2015.

[3] M. A. Fitriady, N. A. Rahmat, and A. F. Mohammad, "*Quasi-Atmospheric Boundary Layer Generation and Enhancement by Spires in a Boundary Layer Wind Tunnel: a Review.*"

[4] E. Pomraning, K. Richards, and P. K. Senecal, "Modeling turbulent combustion using a rans model, detailed chemistry, and adaptive mesh refinement," *SAE Tech. Pap.*, vol. 1, 2014, doi: 10.4271/2014-01-1116.

[5] N. A. Rahmat, A. Hagishima, N. Ikegaya, and J. Tanimoto, "Experimental study on effect of spires on the lateral nonuniformity of mean flow in a wind tunnel," *Evergreen*, vol. 5, no. 1, pp. 1–15, Mar. 2018, doi: 10.5109/1929670.

[6] N. A. Rahmat, A. Hagishima, and N. Ikegaya, "An experimental study on aerodynamic interaction between a boundary layer generated by a smooth and rough wall and a wake behind a spire," vol. 37, no. 2, pp. 19–26, 2016.

[7] J. Counihan, "An improved method of simulating an atmospheric boundary layer in a wind tunnel," *Atmos. Environ.*,

vol. 3, no. 2, pp. 197–214, Mar. 1969, doi: 10.1016/0004-6981(69)90008-0.

[8] J. Armitt and J. Counihan, "The simulation of the atmospheric boundary layer in a wind tunnel," *Atmos. Environ.*, vol. 2, no. 1, pp. 49–71, Jan. 1968, doi: 10.1016/0004-6981(68)90019-x.

[9] H. Kozmar, "Surface pressure on a cubic building exerted by conical vortices," *J. Fluids Struct.*, vol. 92, p. 102801, 2020, doi: 10.1016/j.jfluidstructs.2019.102801.

[10] H. Kozmar and B. Laschka, "Wind-tunnel modeling of wind loads on structures using truncated vortex generators," *J. Fluids Struct.*, vol. 87, pp. 334–353, 2019, doi: 10.1016/j.jfluidstructs.2019.03.007.